

On the Flip Side: Identifying Counterexamples in Visual Question Answering

Gabriel Grand Aron Szanto

School of Engineering and Applied Sciences, Harvard University

Abstract

Visual question answering (VQA) models respond to open-ended natural language questions about images. While VQA is an increasingly popular area of research, it is unclear to what extent current VQA architectures learn key semantic distinctions between visually-similar images. To investigate this question, we explore a reformulation of the VQA task that challenges models to identify counterexamples: images that result in a different answer to the original question. We introduce two plug-and-play methods for evaluating existing VQA models against a supervised counterexample prediction task, VQA-CX. While our models surpass existing benchmarks on VQA-CX, we find that the multimodal representations learned by an existing state-of-the-art VQA model contribute only marginally to performance on this task. These results call into question the assumption that successful performance on the VQA benchmark is indicative of general visual-semantic reasoning abilities.

1. Introduction

Visual question answering (VQA) is an increasingly popular research domain that unites two traditionally disparate AI subfields: natural language processing and computer vision. The goal of VQA is to generate a natural language answer to a question about an image. While a number of existing approaches perform well on VQA (Gupta, 2017; Wu et al., 2017), it is unclear to what extent these models learn key semantic distinctions between visually-similar images.

In this work, we explore a reformulation of the VQA task that more directly evaluates a model’s capacity to reason about the underlying concepts encoded in images. Under the standard VQA task, given the question “What color is the fire hydrant?” and an image of a street scene, a model might answer “red.” Under the alternative task, the model must produce a counterexample; e.g., an image of a fire hydrant that is not red. Successful performance on this task, which we call VQA-CX, requires reasoning about how subtle visual differences between images affect the high-level semantics of a scene.



Figure 1. Counterexample task. The goal is to identify the ground truth counterexample (green border) from a set of 24 visually-similar nearest neighbor images.

Counterexample prediction and VQA are essentially two sides of the same coin. In their paper introducing the VQA 2.0 dataset, Goyal et al. (2016) also propose counterexample identification as a useful explanation modality for VQA models. However, this idea has gone ignored by the VQA research community for two reasons. First, the annual VQA Challenge, which features a public leaderboard, incentivizes researchers to optimize their models to compete on the original task. Second, counterexample prediction requires using the VQA dataset in a non-standard way. While all the data necessary for VQA-CX is publicly available, some non-trivial data wrangling is needed to produce a dataset suitable for training supervised models. To our knowledge, this work represents the first follow-up attempt to operationalize the VQA-CX paradigm originally proposed by Goyal et al. (2016).

We introduce two novel plug-and-play methods for evaluating the performance of existing, pre-trained VQA models on VQA-CX. The first method is an unsupervised model that requires no training and works out-of-box with a pre-trained VQA model. The second method is a supervised neural model that can be used with or without a pre-trained VQA model. The unsupervised model outperforms the baselines proposed in Goyal et al. (2016). Meanwhile, the supervised model outperforms all existing unsupervised

and supervised methods for counterexample prediction.

Crucially, while we use a state-of-the-art VQA model to facilitate counterexample prediction, we find that our methods perform almost as well without receiving any information from this model. In other words, the multimodal representation learned by the VQA model contributes only marginally to performance on VQA-CX. These results challenge the assumption that successful performance on VQA is indicative of more general visual-semantic reasoning abilities.

2. Background

The recent research interest in VQA began with the release of DAQUAR, the DATaset for QUestion Answering on Real-world images (Malinowski & Fritz, 2014). Since then, at least five other major VQA benchmarks have been proposed. These include COCO-VQA (Ren et al., 2015), FM-IQA (Gao et al., 2015), VisualGenome (Krishna et al., 2017), Visual7w (Zhu et al., 2016), and VQA (Antol et al., 2015; Goyal et al., 2016). With the exception of DAQUAR, all of the datasets use include images from the Common Objects in Context (COCO) dataset (Lin et al., 2014), which contains 330K images.

The VQA dataset was first introduced in Antol et al. (2015) as more free-form, open-ended VQA benchmark. Previous datasets placed constraints on the kinds of questions authored by human annotators (e.g., Visual7w, VisualGenome), or relied on image captioning models to generate questions (e.g., COCO-VQA). In contrast, the crowdsourcing method employed by Antol et al. (2015) was designed generate a more diverse range of question types requiring both visual reasoning and common knowledge. However, owing in part to the lack of constraints on question generation, the original VQA dataset contains several conspicuous biases. For instance, “tennis” is the correct answer for 41% of the questions beginning with the phrase, “What sport is...” Additionally, question generation was impacted by a visual priming bias (Zhang et al., 2016), which selected for questions with affirmative answers. For instance, for questions beginning with “Do you see a...,” the correct answer is “yes” 87% of the time. Models that exploit these biases can achieve high accuracy on VQA without understanding the content of the accompanying images (Goyal et al., 2016).

In an effort to balance the VQA dataset, Goyal et al. (2016) introduced VQA 2.0, which is built on pairs of visually-similar images that result in different answers to the same question. Specifically, for each image I in the original dataset, Goyal et al. (2016) determined the 24 nearest neighbor images $I_{NN} = \{I'_1, \dots, I'_{24}\}$ using convolutional image features V derived from VGGNet (Simonyan

& Zisserman, 2014). For each image/question/answer pair (I, Q, A) in the original VQA dataset, crowd workers asked to select a complementary image $I^* \in I_{NN}$ that produced a different answer A^* for the same Q . The most commonly selected I^* was then included as a new example (I^*, Q, A^*) in VQA 2.0, resulting in a dataset that is roughly double the size of the original. In addition to reducing language biases in the data, the pair-based composition of VQA 2.0 provides a convenient approach for supervised training and evaluation of counterexample prediction models.

While the complementary pairs data in VQA 2.0 makes it possible to formalize counterexample prediction as its own machine learning task, several idiosyncrasies in the data make VQA-CX a partially ill-posed problem.

- There may be multiple images in I_{NN} that could plausibly serve as counterexamples. This phenomenon is particularly evident for questions that involve counting (e.g., for $Q =$ “How many windows does the house have?” the majority of images in I_{NN} are likely to contain a different number of windows than the original image.) Consequently, there is no guarantee that the crowd-selected I^* is the only, or even the best, counterexample.
- For approximately 9% of the examples, the answer A^* is the same as A . This irregularity is due to the fact that the tasks of identifying counterexamples and assigning answer labels were assigned to different groups of crowd workers (Goyal et al., 2016). In addition to potential inter-group disagreement, the later group had no way of knowing the intentions of the former. This discontinuity resulted in a subset of degenerate ground truth counterexamples.
- The distribution over the rank of I^* within I_{NN} is not uniform; there is a strong bias towards closer nearest neighbors. In the training set, I^* falls within the top 5 nearest neighbors roughly 44% of the time.
- Certain questions require common knowledge that VQA models are unlikely to possess (e.g., “Is this a common animal to ride in the US?”).
- Other questions simply do not admit to the counterexample task. For instance, given the question, “Do zebras have horses as ancestors?” it is impossible to select an image, zebra or otherwise, that reverses biological fact.

Despite these idiosyncrasies, we demonstrate that it is possible to train supervised models on VQA-CX. However, we found that these quirks of the data adversely affected the performance of our models in ways addressed further in the Discussion.

3. Related Work

To our knowledge, the only published work on the VQA-CX task was carried out by the authors of the VQA 2.0 dataset. Goyal et al. (2016) present a two-headed VQA model that both answers questions about images, and also provides counterexamples. The model consists of a shared base that uses an LSTM and a CNN to embed Q and I , respectively, combining these vectors into a joint embedding QI with pointwise multiplication, as in (Lu et al., 2015). The QI embedding serves as input to two heads: one that produces the answer, and another that picks counterexamples.

In the answering head, QI is passed through a fully-connected layer and fed into a softmax to produce a distribution $P(\mathcal{A})$ over the set of answers \mathcal{A} , constructed as the top most frequent answers from the training set (where $|\mathcal{A}|$ is a hyperparameter). This layer takes a cross entropy loss induced by the ground truth answer $A \in \mathcal{A}$.

In the counterexample head, QI and A are linearly projected into a common embedding space to produce a scalar score $S(I) = QI \cdot A$. This process is repeated for each candidate counterexample image $I'_i \in I_{NN}$ to produce $K = 24$ scores $\mathcal{S} = S(I'_1), \dots, S(I'_{24})$. The scores are passed through a final $K \times K$ fully-connected layer, presumably to allow the model to learn the distribution over the rank of I^* within I_{NN} . The K candidate images are then sorted according to the scores from this final layer. This component is trained with a pairwise hinge ranking loss $\mathcal{L}(\mathcal{S}) = \sum_{I'_i \neq I^*} \max(0, M - (S(I^* - I'_i)))$. This loss formulation, which is similar to the discriminative loss described in Chopra et al. (2005), encourages the model to score the ground-truth counterexample I^* more highly than the other candidates.

In addition to their counterexample model, Goyal et al. (2016) introduce several key baselines for VQA-CX:

- **Random Baseline:** Rank I_{NN} randomly.
- **Distance Baseline:** Rank I_{NN} by L2 distance from I .
- **Hard Negative Mining:** Use a VQA model to determine the probability of the original answer $P(A)_i = \text{VQA}(I'_i, Q)$ for each nearest neighbor $I'_i \in I_{NN}$. Rank the I'_i according to *negative* probability $-P(A)_i$. In other words, choose counterexamples for which the VQA model assigns a low probability to the original answer.

In order to establish a basis for comparison with Goyal et al. (2016), we began by reproducing these three baselines. We then developed two novel models for VQA-CX.

4. Models

As in Goyal et al. (2016), we treat VQA-CX as a supervised learning problem, which can be formalized as follows. For each image, question, and answer (I, Q, A) in the original VQA task, the model is presented with the $K = 24$ nearest neighbor images $I_{NN} = \{I'_1, \dots, I'_{24}\}$ of the original image. The model assigns scores $\mathcal{S} = S(I'_1), \dots, S(I'_{24})$ to each candidate counterexample. The crowd-selected counterexample $I^* \in I_{NN}$ serves as ground truth. For notational clarity, we distinguish between raw images I and convolutional image features V .

Both of our VQA-CX models use an existing VQA model as a submodule. While there exist many diverse solutions for VQA (Wu et al., 2017), we mostly treat the VQA model as a black box. We assume only two aspects of the VQA model’s architecture: (1) The model outputs a distribution $P(A)$ over a discrete number of answer classes, and (2) The model internally produces some multimodal embedding vector Z .¹ We therefore treat a VQA model as a function $\text{VQA}(I, Q) = P(\mathcal{A}), Z$.

We present two architectures for VQA-CX. Both models can be used in conjunction with any VQA model that meets the above two criteria. The first architecture, which we call the Semantic Model, compares the semantic similarity between candidate answers in an embedding space, weighing different answers according to their probability as determined by a VQA model. Since this model relies solely on a pre-trained VQA model and a pre-trained answer embedding, it is fully unsupervised and requires no training. The second architecture is a straightforward multilayer perceptron that takes as input features related to I, I', Q , and A , including the outputs of a VQA model, and returns a score $S(I')$. This NeuralCX model is trained in a pairwise fashion using standard supervised learning methods.

4.1. Unsupervised Semantic Model

The VQA-CX task involves an inherent linguistic tension: while the answer to the counterexample is different from the answer to the original question, the two answers are ideally semantically similar. For example, for the question-answer pair (“What animal is in the tree?”, “cat”) it is more likely that an image with the answer “dog” is the correct counterexample than one with the answer “meatball”, even though “cat” and “meatball” are more semantically unrelated. A successful VQA-CX model will take into account the semantic orthogonality of counterexample answers.

¹(1) While the top models generally treat VQA as a discrete classification task, some models adopt a generative approach (e.g., Wu et al. (2016); Zhu et al. (2015); Wang et al. (2017)), which is not compatible with this assumption. (2) Note that the second assumption, which violates the black box principle, is only used optionally in the NeuralCX model.

The semantic model balances the goal of identifying a semantically similar counterexample answer with the necessity that the answer not be identical to the original. The model takes in a pre-trained VQA model and a pre-trained answer embedding W_A and assigns a score $S(I'_i)$ to each nearest neighbor image:

$$S(I'_i) = \lambda \sum_{a \in \mathcal{A}; a \neq A} \text{cossim}(a, A) P(a) - (1 - \lambda) \log P(a) \quad (1)$$

where cossim is the cosine similarity operator over answer embeddings and $P(a)$ denotes the probability mass that the VQA model places on the answer $a \in \mathcal{A}$ for inputs I' and Q . In this way, the score associated with a candidate is higher if its predicted answer is semantically similar to the original answer and lower if its answer is exactly the same as its original answer. The Semantic Model thus incentivizes candidates with answers that are antonymous to the original answer.

4.2. Supervised NeuralCX Model

The NeuralCX model is a multilayer perceptron that takes as input 10 features derived from I , I' , Q , and A . Some of these features, such as V , Q , and A , are representations of the original image, question, and answer. Others, such as Z and $P(A)$, are computed by a VQA model. Table 1 summarizes the input features.

All features are concatenated into a single input vector \mathbf{v}_{in} and passed through a series of hidden layers, where the size h and number N of layers are variable hyperparameters. All hidden layers share the same h , and use ReLU activation. The output of the last hidden layer is passed through a final linear layer to produce an unnormalized scalar score $S(I')$. Fig. 2 depicts the NeuralCX architecture.

A single training iteration for NeuralCX consists of K forward passes of the network to produce a score for each candidate $I'_i \in I_{NN}$. We compute the cross-entropy loss for the ground truth I^* , and update the parameters of the network via backpropagation.

5. Methods

Our VQA-CX dataset consists of 211K training examples and 118K test examples, of which 10K were reserved as a validation set. A single example in our dataset consists of the original VQA 2.0 example (I, Q, A) , and the 24 nearest neighbor images I_{NN} , which contain the ground truth counterexample $I^* \in I_{NN}$ and its corresponding answer A^* .

Our train and test data are, by necessity, proper subsets of the VQA 2.0 training and validation datasets, respectively. To construct our trainset, we first identified the examples

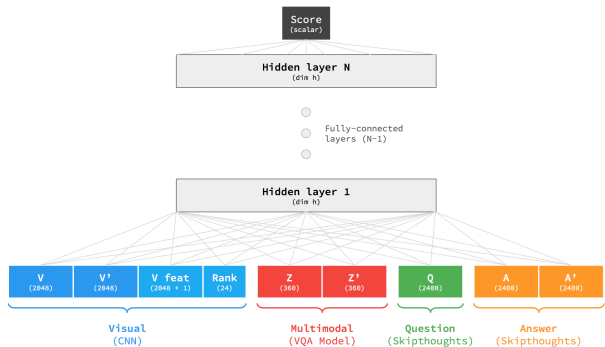


Figure 2. Diagram of NeuralCX architecture. The model is a multilayer perceptron that takes visual, question, answer, and multimodal features as input and produces a score indicating the relevance of I' as a counterexample.

FEATURE	DEFINITION	SIZE	ORIGIN
V	$\text{CNN}(I)$	2048	CNN
V'	$\text{CNN}(I')$	2048	CNN
V_M	$V \odot V'$	2048	COMPUTED
V_D	$\ V' - V\ $	1	COMPUTED
RANK	$\text{ONEHOT}(i)$	24	COMPUTED
Q	$\text{LSTM}(Q)$	2400	LSTM
A	$W_A A$	2400	A_{EMB}
A'	$(W_A)^T P(A')$	2400	$A_{\text{EMB}}, \text{VQA}$
Z	$\text{VQA}(I, Q)$	360	VQA
Z'	$\text{VQA}(I', Q)$	360	VQA

Table 1. Full set of features input to NeuralCX model.

for which the image I had a corresponding I^* . Approximately 22% of the images in VQA 2.0 do not have a labeled complement. These images correspond to instances in which crowd workers indicated that it was not possible to select a counterexample from among I_{NN} (Goyal et al., 2016). Next, we filtered out examples for which I^* did not appear in I_{NN} . Since we used the same list of nearest neighbor images provided by Goyal et al. (2016), I^* should theoretically always appear in I_{NN} . However, because the KNN relation is not symmetric (i.e., $I^1 \in I_{NN}^2 \not\Rightarrow I^2 \in I_{NN}^1$), we found that in certain cases, $I^* \notin I_{NN}$. After filtering, we were left with 211,626/433,757 train examples and 118,499/214,354 validation examples. Note that while Goyal et al. (2016) collected labeled counterexamples for the VQA 2.0 dataset, this data is not public (presumably since it could enable cheating on the VQA 2.0 Challenge). As a result, we did not make use of the VQA 2.0 testset.

We implemented our models and experiments in Pytorch (Paszke et al., 2017). For all experiments involving VQA models, we used MUTAN (Ben-younes et al., 2017), a

state-of-the-art VQA model that uses a Tucker decomposition to parametrize a bilinear interaction between Q and V . We pretrained MUTAN separately on VQA 2.0 for 100 epochs with early stopping to a peak test accuracy of 47.70.² We used a pretrained ResNet-152 model (He et al., 2015) to precompute visual features for all images, and a pretrained Skip-Thoughts model (Kiros et al., 2015) to compute question and answer embeddings. We also utilized framework code from the `vqa.pytorch` Github repository.³

For all experiments with the NeuralCX model, we trained for a maximum of 20 epochs with early stopping. We optimize the model parameters with standard stochastic gradient descent methods, using the Pytorch library implementation of Adam (Kingma & Ba, 2014) with learning rate $1e-4$ and batch size 64. We also employed dropout regularization ($p = 0.25$) between hidden layers (Srivastava et al., 2014).

We experimented with different numbers of hidden layers $N = 1, 2, 3$ and hidden units $h = 256, 512, 1024$, but found that larger architectures resulted in substantial training time increases with negligible performance gains. We therefore use a moderate-sized architecture of $N = 2, h = 512$ for all reported results. This model takes about 35 minutes to train to peak performance on a single Tesla K80 GPU. To ensure determinism, we initialized our random number generators with the same seed before all runs.

We evaluate the performance of our models and baselines with $\text{recall}@k$, which measure the percentage of the ground truth counterexamples that the model ranks in the top k out of the 24 candidate counterexamples. Results on the test set for the NeuralCX Model, Semantic Model, and baseline models are reported in Table 2. To better understand the relative importance of the different inputs to the NeuralCX model, we selectively randomized different features by replacing them with noise vectors drawn from a uniform distribution. Results from these experiments are reported in Table 3.

6. Results

We begin by comparing our baseline results with those of Goyal et al. (2016). As expected, the Random Baseline performed approximately at chance ($\text{recall}@5 \approx \frac{5}{24}$ or 0.2083). Our Distance Baseline is comparable with, but slightly higher than, the result reported in Goyal et al.. This

²Because we needed to train MUTAN on only the VQA 2.0 trainset (and not the valset), the accuracy of our MUTAN model is lower than the best reported results for this model. Additionally, since the VQA-CX task requires us to simultaneously load all 24 V_{NN} features, we opted to save on memory by using a lower-performing no-attention variant of MUTAN.

³<https://github.com/Cadene/vqa.pytorch>

discrepancy indicates that it is possible that the distribution over the rank of the ground-truth counterexample is more skewed in our dataset than in the one used by Goyal et al.. Notably, in both cases, the strategy of ranking counterexample images based on distance in feature space is more than two times better than chance, and serves as a strong baseline.

As in Goyal et al., we found Hard Negative Mining to be a relatively under-performing approach. Since we used a different VQA model from Goyal et al., our results on this baseline are not directly comparable. Nevertheless, in both cases, Hard Negative Mining performed only marginally above chance. To isolate the impact of the VQA model, we computed the Hard Negative Mining baseline with an untrained VQA model. After this change, the performance dropped to random.

The Semantic Model performed between Hard Negative Mining and the Distance Baseline. Interestingly, the value of λ that maximized performance was 1.0, meaning that integrating the overt probability of A under the VQA model only hurt accuracy. We observed a smooth increase in performance as we varied λ between 0 and 1. Clearly, there is some signal in the relative position of the candidate answer embeddings around the ground truth answer, but not enough to improve on the information captured in the visual feature distance.

The NeuralCX model significantly outperformed both the Distance Baseline and the two-headed model from Goyal et al. (2016). To quantify the impact of the VQA model on the performance of NeuralCX, we tested three conditions for the underlying VQA model: untrained, pretrained, and trainable. In the first condition, we initialized NeuralCX with an untrained VQA model. In the second condition, we initialized NeuralCX with a pretrained VQA model, which was frozen during training. In the third, we allowed gradients generated by the loss layer of NeuralCX to backpropagate through the VQA model. We found that fine-tuning the VQA model in this manner produced small gains over the pretrained model. Meanwhile, with an untrained VQA model, the $\text{recall}@5$ of NeuralCX was only 2.39 points lower than with a trained model.

In the NeuralCX randomization experiments, we found that visual features were crucial to strong performance. Without any visual features, recall fell below the Distance Baseline. Both V and the rank embedding appear to be especially important to the task. Intriguingly, these features also appear to be interdependent; randomizing either V or the rank embedding was almost as disruptive as randomizing both. Meanwhile, we found that randomizing the non-visual features produced a much smaller impact. While randomizing A resulted in a small performance drop, randomizing Q and Z did not affect performance at all.

Identifying Counterexamples in VQA

CX MODEL	VQA MODEL	OUR RESULTS		GOYAL ET AL. (2016)
		RECALL@1	RECALL@5	RECALL@5
RANDOM BASELINE	-	4.20	20.85	20.79
HARD NEGATIVE MINING	UNTRAINED	4.06	20.73	-
HARD NEGATIVE MINING	PRETRAINED	4.34	22.06	21.65
SEMANTIC MODEL	UNTRAINED	4.20	21.02	-
SEMANTIC MODEL	PRETRAINED	7.77	30.26	-
DISTANCE BASELINE	-	11.51	44.48	42.84
<hr/>				
TWO-HEADED CX (GOYAL ET AL.)	TRAINABLE	-	-	43.39
NEURALCX	UNTRAINED	16.30	52.48	-
NEURALCX	PRETRAINED	18.27	54.87	-
NEURALCX	TRAINABLE	18.47	55.14	-

Table 2. Results of VQA-CX models and baselines. Where applicable, we compare our results with those reported in Goyal et al. (2016). The midline separates models that are evaluated without training (above) with those that are trained on the VQA-CX dataset (below).

PERFORMANCE		FEATURES RANDOMIZED							
R@5	R@1	V	V _M	V _D	RANK	Q	A	Z	
43.05	12.33	×	×	×	×				
44.48	11.42	×							
44.48	11.51		×	×	×				
44.48	11.52	×	×	×		×	×	×	
44.55	13.17				×				
47.09	13.29					×	×	×	
52.18	16.48						×		
54.87	18.27					×			
54.87	18.27							×	
54.87	18.27							×	

Table 3. Selective randomization of NeuralCX inputs. Features that are marked × are replaced with noise. Randomizations are sorted from top to bottom in order of disruptiveness, with the bottom row showing results from an undisturbed model. The different features are defined in Table 1.

7. Discussion

Our results highlight both promises and challenges associated with VQA-CX. On the one hand, the fact that NeuralCX outperforms the previous best methods suggests that there is room for improvement on this task. This is especially important in light of the pronounced skew in the distribution over the rank of I^* in the dataset, which makes approaches based merely on image distance unreasonably dominant. Given that the supervised neural model from Goyal et al. (2016) barely surpasses their Distance Baseline, it seems likely that this model overfits to the I^* rank distribution. Indeed, since the final $K \times K$ fully-connected layer in this model effectively acts as an information bottleneck, it is unlikely that this network learns anything other than the proper activation biases of the K output units.

In contrast, while we found image distance to be a key feature for NeuralCX, we also find that semantic information about the question and answer are also important sources

of signal. When provided with only visual features, the recall@5 for NeuralCX was 7.78 percentage points lower than when the model was provided with both visual and semantic features (Table 3). In particular, the answer embedding provides information about the semantic similarity between A' and A , which we hypothesize allows the model to select counterexamples that are semantically distinct from the original example. The strong performance of the Semantic Model—which bases its predictions solely on answer similarity, and does not model image distance—also supports this hypothesis. Thus, while visual similarity remains a crucial feature for VQA-CX, our findings demonstrate that in order to achieve peak performance on this task, a model must also leverage semantic information.

While our results show that the answer embedding encodes task-relevant information, the same cannot be said for the multimodal embeddings Z produced by the VQA model. In our randomization experiments, we found that Z and Z' with noise did not affect the performance of NeuralCX. Since Z is, by definition, a joint embedding of Q and V , it is possible that Z does not improve performance because it encodes redundant information. However, if this were the case, we would expect Z to help the model in cases where visual features are not available. Instead, we see a significant drop in accuracy when we randomize the visual features but leave Z , suggesting that the model does not recover visual information from Z .

In general, our findings suggest that the VQA model does not provide NeuralCX with useful information for identifying counterexamples. Replacing the pretrained VQA model with an untrained version only results in a decrease of 2.39 recall@5. (This performance hit is due to the loss of $P(A)$, which is used to weight A'). One could argue that it is unfair to expect the VQA model to provide useful information for VQA-CX, since it was not trained on this task. However, when we co-train the VQA model with

Identifying Counterexamples in VQA

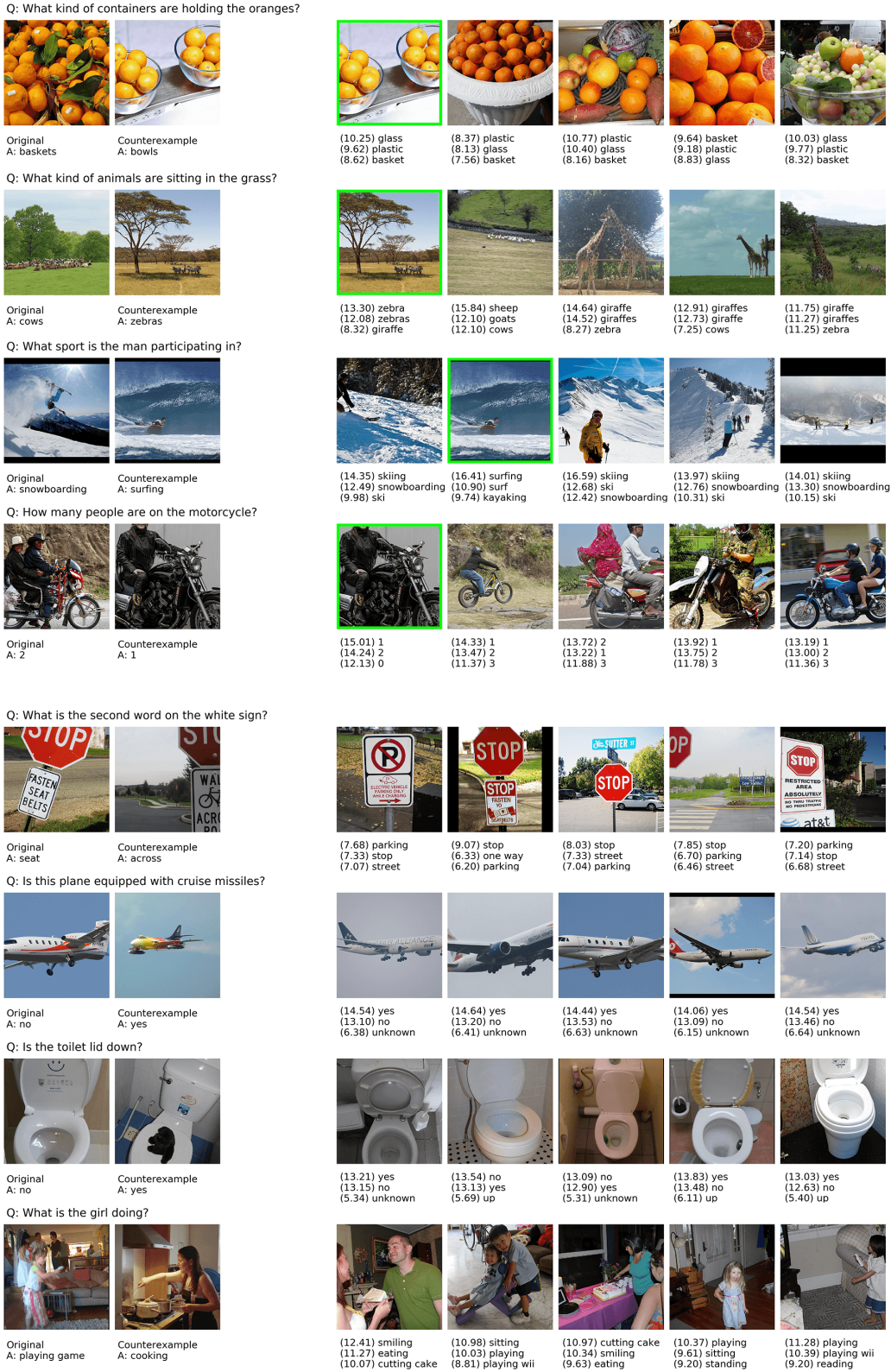


Figure 3. Qualitative results on the counterexample prediction task. Left: The original image and ground truth counterexample from VQA 2.0, along with the question and ground truth answers. Right: the top 5 counterexamples selected by NeuralCX, with the top 3 answers (as scored by a VQA model) underneath. In the top 4 rows, the model correctly identifies the correct counterexample (green outline). In the bottom 4 rows, the model fails. See the Discussion for a review of common failure modes.

NeuralCX, we find only a small performance improvement compared to the pre-trained model. This result holds regardless of whether the VQA model is initialized from pre-trained weights during co-training.

The transfer failure from VQA to VQA-CX raises questions about the extent to which models that perform well on the VQA dataset actually learn semantic distinctions between visually-similar images. In our experiments, we found that while the VQA model often produces the correct answer to a question about an image, it also assigns high probability to semantically-opposite answers. For instance, when answering “yes,” the model’s other top guesses are almost always “no” and “unsure.” Similarly, for questions involving counting, the VQA model often hedges by guessing a range of numbers; e.g., “1, 2, 3” (see Fig. 3). While this strategy may be optimal for the VQA task, it suggests that the VQA model is effectively memorizing what types of answers are likely to result from questions and images. In other words, the VQA model does not actually distinguish between the correct answer and other answers that in many cases carry opposite meanings.

While our results expose clear problems with the existing approaches to VQA, it is important to consider two external failure modes that also affect performance on VQA-CX. The first relates to NeuralCX not picking up on information from the VQA model. In some cases, even when the VQA model correctly identified a particular I' as producing the same answer as the original, NeuralCX still chose I' as a good counterexample. In other cases, NeuralCX incorrectly assigned high scores to images for which $A' \approx A$; e.g., an image of children “playing” was selected as a counterexample to an image of children “playing game.” These failures indicate that NeuralCX does not optimally leverage the semantic information in the answers produced by the VQA model, suggesting a promising area for future improvement.

The second failure mode arises from issues with the data itself. In many cases, our models identified valid counterexamples that scored as being incorrect, since only a single $I^* \in I_{NN}$ is labeled as the ground truth. Next, many of the questions in VQA 2.0 require specialized visual reasoning skills that, while within reach for current machine learning methods, are unlikely to be learned by general VQA architectures; e.g., “What is the second word on the sign?” or “What time is on the clock?” Finally, a non-trivial portion of the question require common sense reasoning beyond the scope of contemporary machine learning methods; e.g., “Does this vehicle require gasoline?” or “What kind of liquor is in the green bottle?” These questions may some day be a useful test of artificial general intelligence. However, given the limitations of current AI methods, we feel the inclusion of commonsense questions in VQA 2.0

actually detracts from the task by encouraging strategies that involve little more than educated guessing.

8. Conclusion

In this work, we explored different approaches to counterexample prediction on VQA 2.0. We introduced two plug-and-play architectures for evaluating the performance of existing VQA models on this task. The Semantic Model, which uses weighted answer similarity to score candidate counterexamples, outperforms existing baselines without any training on the VQA-CX task. Meanwhile, the NeuralCX model, which is trained on VQA-CX data in a supervised manner, established a new state-of-the-art for this task. Crucially, both models successfully leverage semantic information about answers in addition to visual features about the images.

While we used a top-performing VQA model in our experiments, we found that representations learned by this model failed to improve performance on the counterexample prediction task. We also observed that the VQA model assigns high probability to answers with opposite meanings. These results suggest that VQA models that perform well on the original task do not necessarily learn conceptual distinctions between visually-similar images. Our findings raise important questions about the effectiveness of VQA as a benchmark of multimodal reasoning.

These issues occur amidst general concerns about AI interpretability. While machine learning has exploded in popularity, the research community has only very recently begin to treat interpretability as a serious issue (Doshi-Velez & Kim, 2017). As machine learning systems assume increasing levels of decision-making responsibility in society, it is imperative that they be able to provide human-interpretable explanations. Within the domain of VQA, explanation by counterexample serves as an useful way for machines to build trust among their users (Goyal et al., 2016). However, this explanation modality will only serve its intended purpose if the underlying systems can represent the underlying concepts encoded in images. Ultimately, counterexample prediction may only be a stepping stone to a test of true understanding. As Einstein once observed, “Imagine is more important than knowledge” (Einstein, 1931). Ultimately, in order to produce a truly convincing counterexample, a machine may need to generate one on its own.

References

- Antol, Stanislaw, Agrawal, Aishwarya, Lu, Jiasen, Mitchell, Margaret, Batra, Dhruv, Zitnick, C. Lawrence, and Parikh, Devi. VQA: visual question answering. *CoRR*, abs/1505.00468, 2015. URL <http://arxiv.org/abs/1505.00468>.

- Ben-younes, Hedi, Cadène, Rémi, Cord, Matthieu, and Thome, Nicolas. MUTAN: multimodal tucker fusion for visual question answering. *CoRR*, abs/1705.06676, 2017. URL <http://arxiv.org/abs/1705.06676>.
- Chopra, Sumit, Hadsell, Raia, and LeCun, Yann. Learning a similarity metric discriminatively, with application to face verification. In *Computer Vision and Pattern Recognition, 2005. CVPR 2005. IEEE Computer Society Conference on*, volume 1, pp. 539–546. IEEE, 2005.
- Doshi-Velez, Finale and Kim, Been. Towards a rigorous science of interpretable machine learning. 2017.
- Einstein, Albert. *Cosmic religion: With other opinions and aphorisms*. Covici-Friede, 1931.
- Gao, Haoyuan, Mao, Junhua, Zhou, Jie, Huang, Zhiheng, Wang, Lei, and Xu, Wei. Are you talking to a machine? dataset and methods for multilingual image question. In *Advances in neural information processing systems*, pp. 2296–2304, 2015.
- Goyal, Yash, Khot, Tejas, Summers-Stay, Douglas, Batra, Dhruv, and Parikh, Devi. Making the V in VQA matter: Elevating the role of image understanding in visual question answering. *CoRR*, abs/1612.00837, 2016. URL <http://arxiv.org/abs/1612.00837>.
- Gupta, Akshay Kumar. Survey of visual question answering: Datasets and techniques. *CoRR*, abs/1705.03865, 2017. URL <http://arxiv.org/abs/1705.03865>.
- He, Kaiming, Zhang, Xiangyu, Ren, Shaoqing, and Sun, Jian. Deep residual learning for image recognition. *CoRR*, abs/1512.03385, 2015. URL <http://arxiv.org/abs/1512.03385>.
- Kingma, Diederik P. and Ba, Jimmy. Adam: A method for stochastic optimization. *CoRR*, abs/1412.6980, 2014. URL <http://arxiv.org/abs/1412.6980>.
- Kiros, Ryan, Zhu, Yukun, Salakhutdinov, Ruslan, Zemel, Richard S., Torralba, Antonio, Urtasun, Raquel, and Fidler, Sanja. Skip-thought vectors. *CoRR*, abs/1506.06726, 2015. URL <http://arxiv.org/abs/1506.06726>.
- Krishna, Ranjay, Zhu, Yuke, Groth, Oliver, Johnson, Justin, Hata, Kenji, Kravitz, Joshua, Chen, Stephanie, Kalantidis, Yannis, Li, Li-Jia, Shamma, David A, et al. Visual genome: Connecting language and vision using crowd-sourced dense image annotations. *International Journal of Computer Vision*, 123(1):32–73, 2017.
- Lin, Tsung-Yi, Maire, Michael, Belongie, Serge, Hays, James, Perona, Pietro, Ramanan, Deva, Dollár, Piotr, and Zitnick, C Lawrence. Microsoft coco: Common objects in context. In *European conference on computer vision*, pp. 740–755. Springer, 2014.
- Lu, Jiasen, Lin, Xiao, Batra, Dhruv, and Parikh, Devi. Deeper lstm and normalized cnn visual question answering model, 2015.
- Malinowski, Mateusz and Fritz, Mario. A multi-world approach to question answering about real-world scenes based on uncertain input. In *Advances in neural information processing systems*, pp. 1682–1690, 2014.
- Paszke, Adam, Gross, Sam, Chintala, Soumith, and Chanan, Gregory. Pytorch, 2017.
- Ren, Mengye, Kiros, Ryan, and Zemel, Richard. Image question answering: A visual semantic embedding model and a new dataset. *Proc. Advances in Neural Inf. Process. Syst*, 1(2):5, 2015.
- Simonyan, Karen and Zisserman, Andrew. Very deep convolutional networks for large-scale image recognition. *arXiv preprint arXiv:1409.1556*, 2014.
- Srivastava, Nitish, Hinton, Geoffrey, Krizhevsky, Alex, Sutskever, Ilya, and Salakhutdinov, Ruslan. Dropout: A simple way to prevent neural networks from overfitting. *The Journal of Machine Learning Research*, 15(1): 1929–1958, 2014.
- Wang, Peng, Wu, Qi, Shen, Chunhua, Dick, Anthony, and van den Hengel, Anton. Fvqa: Fact-based visual question answering. *IEEE transactions on pattern analysis and machine intelligence*, 2017.
- Wu, Qi, Wang, Peng, Shen, Chunhua, Dick, Anthony, and van den Hengel, Anton. Ask me anything: Free-form visual question answering based on knowledge from external sources. In *Proceedings of the IEEE Conference on Computer Vision and Pattern Recognition*, pp. 4622–4630, 2016.
- Wu, Qi, Teney, Damien, Wang, Peng, Shen, Chunhua, Dick, Anthony, and van den Hengel, Anton. Visual question answering: A survey of methods and datasets. *Computer Vision and Image Understanding*, 163:21–40, 2017.
- Zhang, Peng, Goyal, Yash, Summers-Stay, Douglas, Batra, Dhruv, and Parikh, Devi. Yin and yang: Balancing and answering binary visual questions. In *Computer Vision and Pattern Recognition (CVPR), 2016 IEEE Conference on*, pp. 5014–5022. IEEE, 2016.

Zhu, Yuke, Zhang, Ce, Ré, Christopher, and Fei-Fei, Li. Building a large-scale multimodal knowledge base system for answering visual queries. *arXiv preprint arXiv:1507.05670*, 2015.

Zhu, Yuke, Groth, Oliver, Bernstein, Michael, and Fei-Fei, Li. Visual7w: Grounded question answering in images. In *Proceedings of the IEEE Conference on Computer Vision and Pattern Recognition*, pp. 4995–5004, 2016.